



## Development and characterization of high thermal conductivity magnetic formulation for cryotherapy

Iryna Vedernikova

*Department of Inorganic Chemistry, National University of Pharmacy, Ukraine  
Pushkinskaya St. 53, Kharkov, Ukraine*

---

### ABSTRACT

*In this article a high thermal conductivity magnetic topical medication is provided as a heat transfer agent for cryotherapy. By an appropriate combination of the magnetic formulations prepared using different amounts of magnetite nanoparticles and different type of bases, it was possible to obtain a high thermal conductivity system with a good texture and magnetic properties. Transverse magnetic field increases the thermal conductivity of the formulations to almost two times its initial value. It was found that polyethylene glycol PEG400/PEG1500 mixed base with magnetite nanoparticles (30.0-50.0%) is a promising candidate for cryotherapy.*

**Key words:** Cryotherapy, Magnetite nanoparticles, Thermal conductivity.

---

### INTRODUCTION

Cryotherapy involves the application of cold to freeze and destroy abnormal skin cells that require removal. The application has been extended to the treatment of solid tumors as well as malignant lesions of the skin [1-4]. Successful cryo-treatment requires maximum freezing rate. Sometimes, a second application may be necessary depending on the size of the growth.

Cryotherapy efficiency can be increased significantly with appropriate loading of nanoparticles with high thermal conductivity in target tissues. Injection of nanoparticles with high thermal conductivity serves to enhance the heat transfer rate and regulate the orientation of ice-ball which is highly desirable in treatment of complex irregularly shaped tumors [5-8].

Thermal conductivity is the property of a material to conduct heat. It can be defined as the quantity of heat transmitted through a unit thickness of a material - in a direction normal to a surface of unit area - due to a unit temperature gradient under steady state conditions. Thermal conductivity depends on many properties of a material, notably its microstructure and temperature. Pure crystalline substances exhibit highly variable thermal conductivities along different crystal axes.

Nanofluids are a new class of heat transfer fluids containing nanoparticles of crystalline substances with the size under 100 nm which are suspended in a uniform and stable manner in the base fluid. Energy transportation (e.g. heat transfer) of the nanofluid is affected by the type and properties of the nanoparticles [9]. Nanofluids with magnetic nanoparticles constitute a special class of fluids that exhibit both magnetic and fluid properties, which can be changed by applying an external magnetic field.

In this paper we described the experimental detail for preparation of high thermal conductivity magnetic medication to determine the optimum composition in order to obtain the formulation with good texture and magnetic properties that is needed for topical heat transfer agent for cryotherapy. The magnetite nanoparticles were characterized by transmission electron microscopy (TEM), powder X-ray diffraction (XRD), vibrating sample magnetometry (VSM). The properties of formulations of varying compositions prepared by using different amounts of magnetite nanoparticles and different type of bases were also discussed.

### EXPERIMENTAL SECTION

Iron (III) chloride ( $\text{FeCl}_3 \cdot 6\text{H}_2\text{O}$ ), iron (II) sulfate ( $\text{FeSO}_4 \cdot 7\text{H}_2\text{O}$ ),  $\text{NH}_3 \cdot \text{H}_2\text{O}$  (25% w/w aqueous solution) and polyethylene glycols (PEG) were purchased from E. Merck Ltd. (India). Lugol iodine was purchased from Instamed Labchem (India); sea buckthorn oil from X.S. Biotech Co., Ltd. (China) and oleic acid from Beijing ChemWorks (China). All chemicals were of analytical grade.

#### Synthesis of magnetite nanoparticles

Ultrafine particles of magnetite were prepared by co-precipitating aqueous solutions of iron (II) salt ( $\text{FeSO}_4 \cdot 7\text{H}_2\text{O}$ ) and iron (III) salt ( $\text{FeCl}_3 \cdot 6\text{H}_2\text{O}$ ) in an alkaline medium (25%  $\text{NH}_3 \cdot \text{H}_2\text{O}$ ). 13.89 g (0.05 mol) of  $\text{FeSO}_4 \cdot 7\text{H}_2\text{O}$  and 26.90 g (0.1 mol) of  $\text{FeCl}_3 \cdot 6\text{H}_2\text{O}$  were dissolved in 1 L of distilled water at heating (60-70°C). 25% aqueous ammonia solution was added drop-wise with continuous stirring until complete precipitation of the black ferrite was achieved (pH 9-11). After the system was cooled to room temperature, the precipitates were collected using magnetic separation and washed with distilled water until pH neutral, producing thus samples MNPs.

#### Preparation of formulations

The formulations of varying compositions (Table 1) were prepared by using different amounts of MNPs and different type of bases. The mixture of PEG were prepared by melting together polyethylene glycol (PEG 400 and PEG 1500) on a hot plate/stirrer (at 70°C). The PEG 400/1500 ratios weight were 9/1 (forms I-V) and 4/1 (forms VI-VII), respectively. MNPs were added to this molten base while stirring. The entire mixture was stirred while cooling.

Table 1. Compositions used in the study

Ingredients	Formulations								
	I	II	III	IV	V	VI	VII	VIII	IX
MNPs	20	25	30	35	40	25	30	10	50
PEG 400	72	67.5	63.0	58.5	54.0	60.0	56	-	-
PEG 1500	8	7.5	7.0	6.5	6.0	15.0	14	-	-
Lugol iodine	-	-	-	-	-	-	-	90	-
Sea buckthorn oil	-	-	-	-	-	-	-	-	47.5
Oleic acid	-	-	-	-	-	-	-	-	2.5

#### Characterization techniques

The X-ray diffraction (XRD) patterns of the samples were recorded on a Siemens D500 X-ray powder diffractometer using copper radiation. Slow scans of the selected diffraction peaks were carried out in the step mode (step size 0.03°, measurement time 75 s). The crystallite size of the nanocrystalline samples was measured from the X-ray line broadening using the Debye-Scherrer formula after accounting for instrumental broadening. Magnetization measurements were performed in a vibrating sample magnetometer at 300 K using a superconducting magnet to produce fields up to 2 kOe.

The thermal conductivity was measured in an apparatus based in the use of steady-state method. The schematic diagram of the experimental layout is shown in Figure 1.

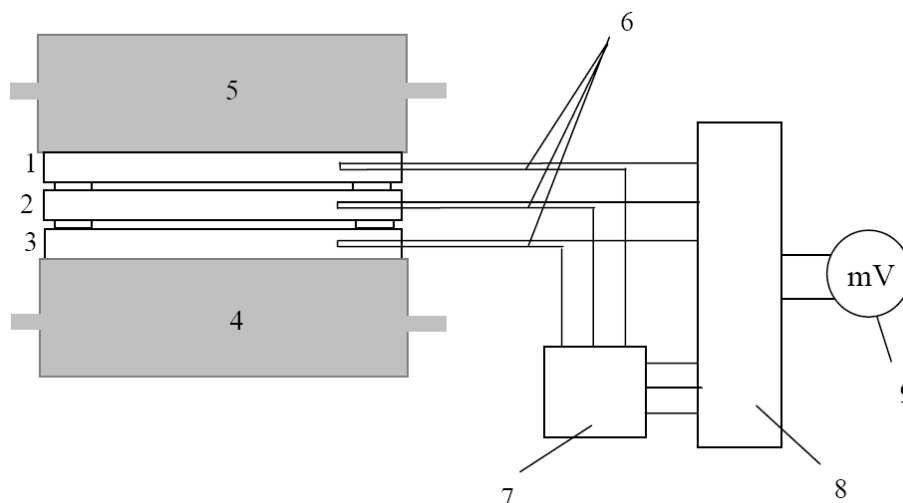


**Figure 1. Schematic diagram of the experimental layout:**  
 1, 2, 3 – brass disks; 4, 5 – constant temperature baths; 6 – thermocouple;  
 7 – Dewar vessel; 8 – remote switch; 9 – digital voltmeter

Samples of unknown thermal conductivity are sandwiched between two brass disks. Each brass disk has a hole where a thermistor can be inserted for temperature measurement. The voltage readings on the recorder chart were exactly proportional to the electromotive force of the thermocouple.

## RESULTS AND DISCUSSION

The XRD results indicate typical X-ray powder diffraction pattern of magnetite nanoparticles (Figure 2). The pattern shows characteristic peaks at  $2\theta=18.2^\circ$ ,  $30.0^\circ$ ,  $35.4^\circ$ ,  $43.0^\circ$ ,  $53.4^\circ$ ,  $56.9^\circ$ ,  $62.5^\circ$ , and  $74.0^\circ$ , marked by (111), (220), (311), (400), (422), (511), (440), and (533) which were indexed in the  $Fd3m(227)$  space group corresponding to a spinel cubic structure of magnetite (JCPDS PDF card no. 19-629).

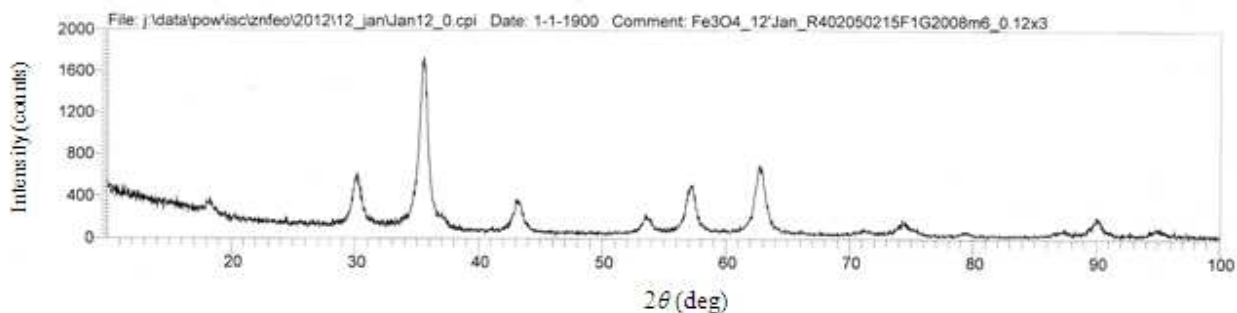


**Figure 2. X-ray diffraction pattern of MNPs**

Taking the highest intensity peak, namely the (311) plane, at  $2\theta = 35.4^\circ$ , and the half maximum intensity width of the peak after accounting for instrument broadening, the calculated particle size is 16.7 nm. The results were in good agreement with the data obtained from XRD and TEM. From TEM images (Figure 3) it is evident that the particles are well separated and almost monodisperse. The size for  $\text{Fe}_3\text{O}_4$  particles is  $17\pm 0.5$  nm.

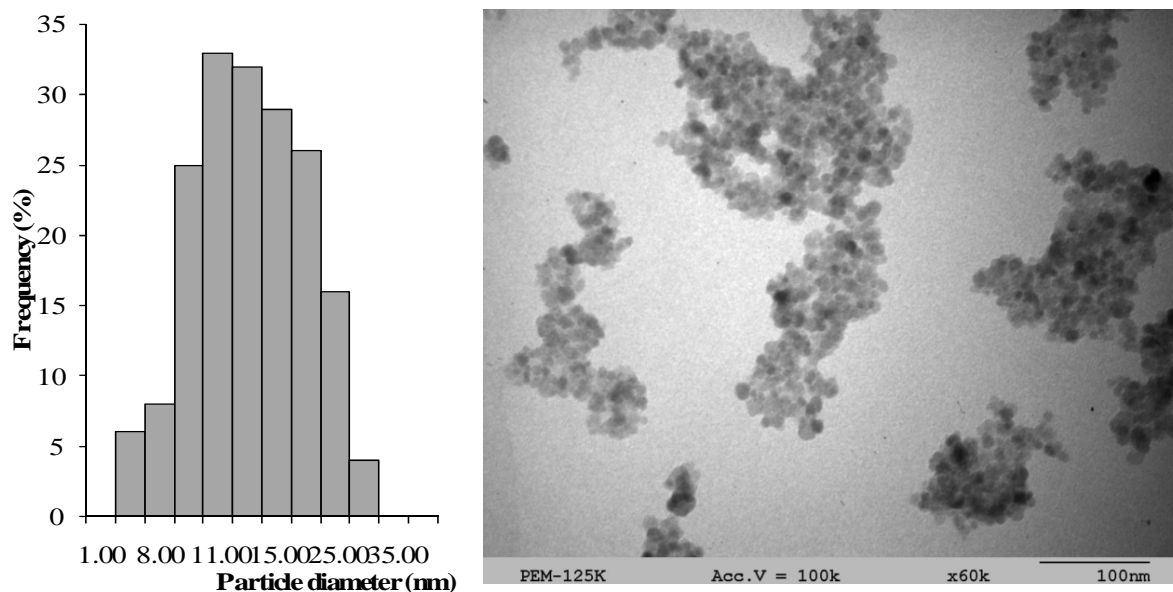


Figure 3. TEM morphologies of MNPs and statistical result of nanoparticles size distribution

The magnetic measurement confirms that the synthesized particles exhibit superparamagnetic properties at room temperature. The magnetization curve for the MNPs exhibits immeasurable values of coercivity field and remnant magnetization. The particles have high saturation magnetization values (67 emu/g), which is consistent with the value reported in the literature for a magnetite sample with the same sizes [10] but lower than bulk magnetite particles of 90 emu/g [11].

It is known that smaller particles (nanoscale magnetite) are less magnetic than the same material in bulk form because they contain a substantially greater fraction of metal ions located on the crystal surface, which may not contribute to the particle's net magnetization [10-12].

The particles of magnetite impart the magnetic properties to the formulations. These properties allow for the rapid and easy manipulation and fixing of the formulation by the application of an external magnetic field. Also, due to these properties the magnetic particles can be exploited as heat conductor, as magnetite has a high value of thermal conductivity ( $9.7 \text{ Wm}^{-1}\text{K}^{-1}$  [13]).

To develop a high thermal conductivity magnetic formulation for cryotherapy, it should possess good texture and magnetic properties, high value of thermal conductivity. The thermal conductivity of the samples ( $\lambda$ ) was calculated from the Maxwell equation:

$$\lambda = \lambda_b \frac{2\lambda_b + \lambda_m + 2\varphi(\lambda_m - \lambda_b)}{2\lambda_b + \lambda_m - \varphi(\lambda_m - \lambda_b)}$$

where  $\lambda_b$  and  $\lambda_m$  are the thermal conductivity of the base and the magnetite, and  $\varphi$  is the volume fraction of magnetite nanoparticles.

Table 2. Parameters and physical characteristics of the formulations

Parameters	Formulations								
	I	II	III	IV	V	VI	VII	VIII	IX
Mass part of magnetite, %	20	25	30	35	40	25	30	10	50
Volume part of magnetite, %	5.35	6.68	8.08	9.43	10.81	6.35	7.87	2.44	12.5
Density, g/cm <sup>3</sup>	1.281	1.320	1.356	1.402	1.432	1.331	1.378	1.271	1.306
Saturation magnetization, emu/g	3.52	4.47	5.32	6.21	36.69	7.09	5.17	1.61	8.16
$\lambda$ , W/(m·K)	0.3041	0.3295	0.3549	0.3803	0.4057	0.3138	0.3278	0.2916	0.2466

The results of comparing of the properties of the proposed compositions (Table 2) showed that the optimum formulations are II – IV because they have the best structure and one of the highest magnetic properties which allowing its manipulation with an external magnetic field and the highest thermal conductivities. Other formulations were not accepted because they have liquefied structure like formulations I, VIII-IX or too dense structures like formulations V-VII. Therefore, the formulations II – IV with the PEG mixture were selected for further study.

The direction of an external magnetic field relative to the temperature gradient affects the energy transport process of the suspended nanoparticles inside the magnetic fluid [14, 15]. The present study was focused on thermal conductivity as a function of various parameters such as volume fraction, magnetic field in transverse and longitudinal directions. The results of two different magnetic field intensities of the formulations II – IV are shown in Figure 4.

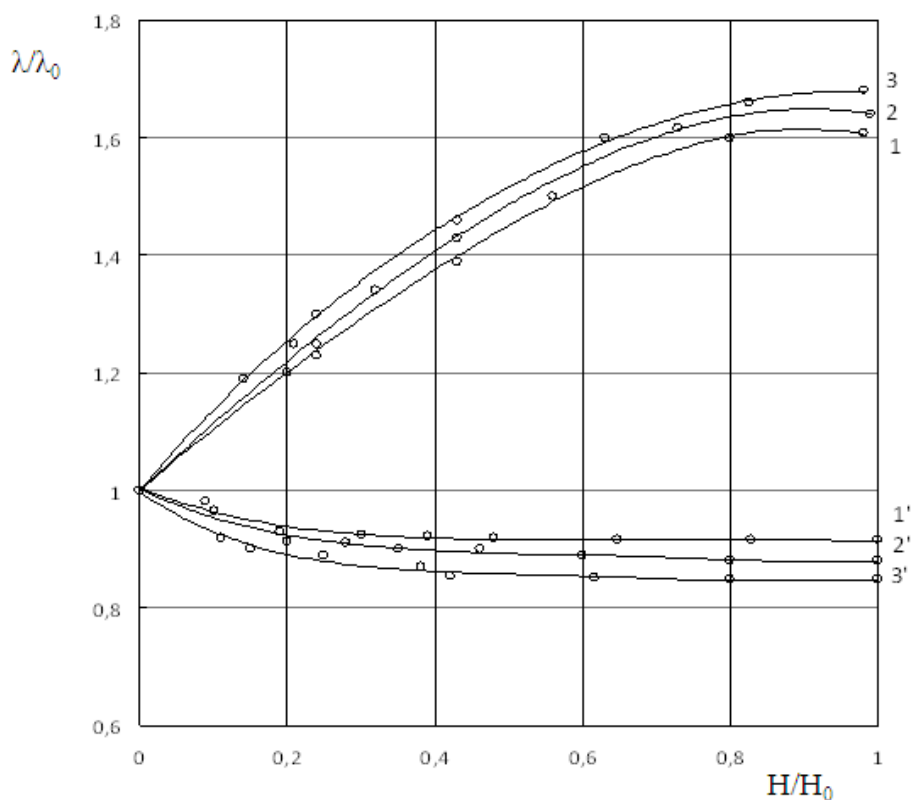


Figure 4. The field dependence of relative effective thermal conductivity, normalized to  $\lambda_0$  – thermal conductivity before applying any magnetic field of the formulations II, III and IV under the influence of transverse (1, 2, 3) and longitudinal (1', 2', 3') magnetic fields

Figure 4 shows the relative effective thermal conductivity, normalized to  $\lambda_0$  – thermal conductivity before applying any magnetic field of the formulations under the influence of transverse and longitudinal magnetic fields. Transverse magnetic field increases the thermal conductivity of the formulations until it reaches a maximum value and then

after a slight decrease a constant value is maintained. Longitudinal magnetic field slightly decreases the thermal conductivity of the samples.

When sufficiently strong transverse magnetic field is applied, the thermal conductivity increases to almost two times its initial value. This behavior can be explained by the presence of chain-like structures in sample with respect to the influence of magnetic field. In the presence of magnetic field, the MNPs tend to align in the direction of the field because of the anisotropy of the susceptibility. The reason for this enhancement was the change of nanostructures induced by the external magnetic field in the formulations. In case of horizontal magnetic field, the formed magnetite particle chains provided the more effectively bridges for energy transport inside the formulation along the direction of temperature gradient and enhanced the thermal process in the sample.

This result is similar to that observed by other researchers [16-19]. The enhancement up to 300% using 6.3% volume fraction of magnetic nanoparticles in kerosene when magnetic field is applied has been reported [18]. Because of the formation of reversible chain under the influence of magnetic field, it shows drastic enhancement in thermal conductivity.

### CONCLUSION

The results presented in this study showed that the PEG-based formulation with 30.0-50.0 % of magnetite nanoparticles can be effectively used as a thermal conductivity agent for cryotherapy. Due to the higher thermal conductivity of the MNPs, the thermal conductivity of the formulation increases proportionally to the content of the nanoparticles. Black color of MNPs formulation during cryosurgery could also help better image the edge of a tumor as well as the margin of the ice ball.

### Acknowledgement

Author gratefully acknowledges Physics Faculty of V. N. Karazin Kharkiv National University (Ukraine) for providing necessary facilities to carry out the research work.

### REFERENCES

- [1] SM Cooper; RP Dawber. *J. Royal Soc. Med.*, **2001**, 94(4), 196-201.
- [2] MD Andrews. *Am. Family Physician*, **2004**, 69(10), 2365-2372.
- [3] AA Gage; JG Baust. *Cryobiology*, **1998**, 37, 171– 186.
- [4] JO Karlsson; M Toner. *Biomaterials*, **1996**, 17, 243-256.
- [5] TH Yu; J Liu; YX Zhou. *Cryobiology*, **2005**, 50, 174-182.
- [6] RK Visaria; RJ Griffin; BW Williams; ES Ebbini; GF Paciotti; CW Song; JC Bischof. *Mol. Cancer. Ther.*, **2006**, 5, 1014-1020.
- [7] YG Lv; J Liu. *Micronanoelectronic Tech.*, **2004**, 41, 22-28.
- [8] S Singh; R Bhargava. *J. Heat Transfer*, **2014**, 136, 101-110.
- [9] A Gavili; M Lajvardi; J Sabbaghzadeh. *J. Computational and Theoretical Nanosci.*, **2010**, 7, 1425-1435.
- [10] GF Goya; TS Berquo; FC Fonseca; MP Morales. *J. Appl. Phys.*, **2003**, 94, 3520-3528.
- [11] Y Yuan; D Rende; CL Altan; S Bucak; R Ozisik; DA Borca-Tasciuc. *Langmuir*, **2012**, 28, 13051-13059.
- [12] P Kucheryavy; J He; VT John; P Maharjan; L Spinu; GZ Goloverda; VL Kolesnichenko. *Langmuir*, **2013**, 29(2), 710-716.
- [13] M. Rob. *Elastomers and Plastics*, **2003**, 6, 322-329.
- [14] K Parekh. *Solid State Communications*, **2014**, 184, 33-37.
- [15] DD Nikodijevic; ZM Stamenkovic; MM Jovanovic; MM Kocic; JD Nikodijevic. *Thermal Sci.*, **2014**, 18(3), 1019-1028.
- [16] K Parekh; HS Lee. *J. Appl. Phys.*, **2010**, 107, 310-312.
- [17] K Shimada; Y Akagami; T Fujita; T Miyazaki; S Kamiyama; A Shibayam. *J. Magn. Magn. Mat.*, **2002**, 252, 235-237.
- [18] J Philip; PD Shima; B Raj. *Appl. Phys. Lett.*, **2007**, 91(20), 31-39.
- [19] JA Eastman; US Choi; S Li; W Yu; LJ Thompson. *Appl. Phys. Lett.*, **2001**, 78(6), 718 – 720.